

Spatially Controlled Suzuki and Heck Catalytic Molecular Coupling

Jason J. Davis,^{*,†} Claire B. Bagshaw,[†] Katerina L. Busuttill,[†] Yuki Hanyu,[†] and Karl S. Coleman[‡]

Contribution from the Department of Chemistry, University of Oxford, Chemistry Research Laboratory, Mansfield Road, OX1 3TA, UK, and Department of Chemistry, University Science Laboratories, South Road, Durham University, DH1 3LE, UK

Received July 7, 2006; E-mail: jason.davis@chem.ox.ac.uk

Abstract: The initiation and control of chemical coupling has the potential to offer much within the context of “bottom up” nanofabrication. We report herein the use of a palladium-modified, catalytically active, AFM probe to initiate and spatially control surface-confined Suzuki and Heck carbon–carbon coupling reactions. These “chemically written reactions”, detectable by lateral force and chemically specific optical and topographic labeling, were patterned with line widths down to 15 nm or ~ 20 molecules. Catalyzed organometallic coupling was, in this way, carried out at subzeptomolar levels. By varying the catalyst–substrate interaction times, turnover numbers of $(0.6–1.2) \times 10^4$ and $(3.0–5.0) \times 10^4$ molecules s^{-1} were resolved for Suzuki and Heck reactions, respectively.

Introduction

The generation of patterned surfaces has attracted considerable attention during the past decade, due to significant and varied potential application in optoelectronics, sensory technology, and the electronics industry.^{1–5} Current methods of patterning molecular functionality at the nanometer scale rely heavily on mechanical displacement,^{6–8} oxidation,^{9,10} or direct molecular delivery methods;¹¹ mechanical nanolithography, or “nanoshaving”, for example, typically involves the controlled removal of molecules from a monolayer using appropriate forces imparted by an atomic force (AFM) or scanning tunneling microscope (STM) probe.^{7,8,12} AFM tips have, additionally, been used to deliver molecules to a surface in a pattern defined by the boundaries of the scan.^{13–15} Although one can envisage the use

of AFM probes, in ambient atmosphere, to initiate reactions on a surface through “molecular delivery”, such an approach offers rather limited scope for either control or flexibility.

Previous reports of AFM probe-induced reactions involve simple reduction, hydrogenation, or hydrolysis. Müller et al. presented a platinum-coated probe-catalyzed hydrogenation of self-assembled monolayers (SAMs) of alkyl azides to alkylamines.¹⁶ McDonald et al. have similarly demonstrated a localized terminal azide reduction using palladium-coated probes.¹⁷ Probe-mediated borohydride reduction and acid hydrolysis reactions have also been reported.^{18,19} Although developmentally significant, none of these procedures directly couple surface bound and fluid-phase reagents in a way that is instantly amenable to nanofabrication by molecular assembly. We demonstrate, herein, that, by catalytically modifying an AFM probe, surface-confined carbon–carbon catalytic coupling reactions can be induced and utilized in chemically altering the terminal functionality of a reagent SAM at nanometer levels of lateral resolution.

The Suzuki coupling reaction is a simple synthetic route to the fabrication of biaryls from aryl halides and aryl boronic acids in the presence of a palladium catalyst and base.²⁰ Concomitant displacement of boron fragments and halogens occurs.²¹ This cross-coupling reaction can be used to couple a wide range of reagents and, hence, has many potential applications, including

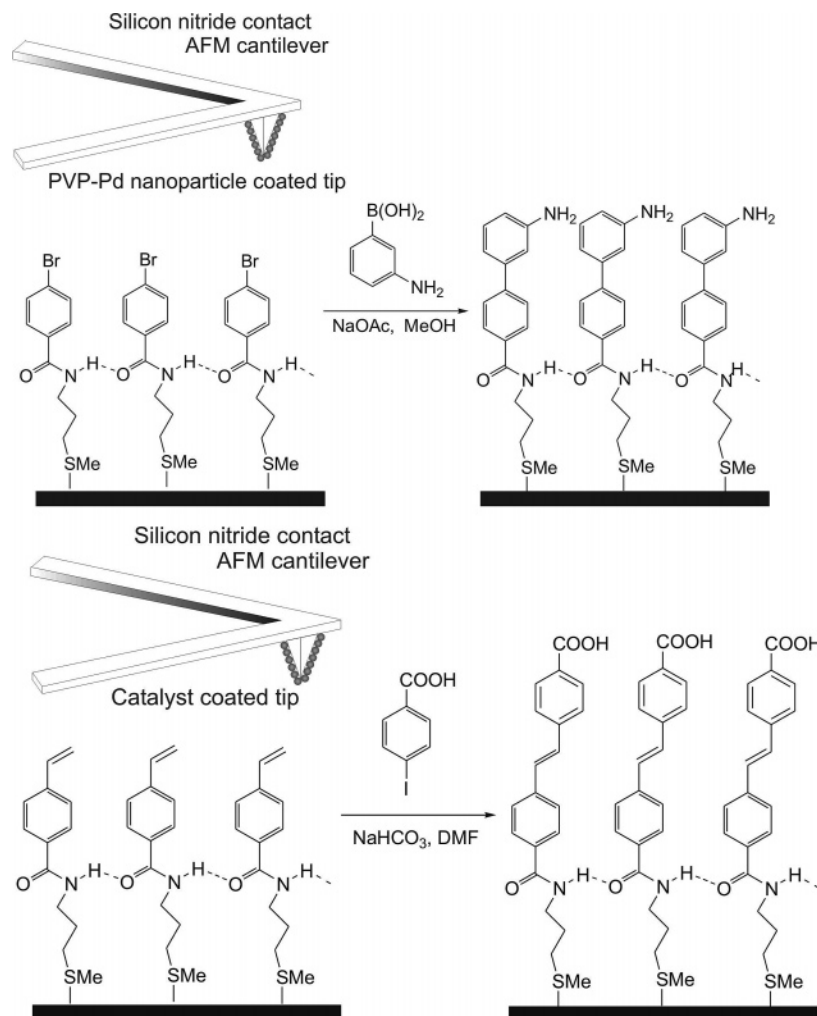
[†] University of Oxford.

[‡] Durham University.

- (1) Lang, H. P.; Hegner, M.; Meyer, E.; Gerber, C. *Nanotechnology* **2002**, *13*, R29–R36.
- (2) Colton, R. J.; Baselt, D. R.; Dufrene, Y. F.; Green, J.-B. D.; Lee, G. U. *Curr. Opin. Chem. Biol.* **1997**, *1*, 370–377.
- (3) Poggi, M. A.; Gadsby, E. D.; Bottomley, L. A.; King, W. P.; Oroudjev, E.; Hansma, H. *Anal. Chem.* **2004**, *76*, 3429–3443.
- (4) Su, M.; Li, S.; Dravid, V. P. *J. Am. Chem. Soc.* **2003**, *125*, 9930–9931.
- (5) Bottomley, L. A. *Anal. Chem.* **1998**, *70*, 425R–475R.
- (6) Headrick, J. E.; Armstrong, M.; Cratty, J.; Hammond, S.; Sheriff, B. A.; Berrie, C. L. *Langmuir* **2005**, *21*, 4117–4122.
- (7) Leggett, G. J. *Analyst* **2005**, *130*, 259–264.
- (8) Liu, G. Y.; Xu, S.; Qian, Y. *Acc. Chem. Res.* **2000**, *33*, 457–66.
- (9) Chien, F. S. S.; Hsieh, W. F.; Gwo, S.; Vladar, A. E.; Dagata, J. A. *J. Appl. Phys.* **2002**, *91*, 10044–10050.
- (10) Tello, M.; Garcia, F.; Garcia, R. *J. Appl. Phys.* **2002**, *92*, 4075–4079.
- (11) Zhang, H.; Mirkin, C. A. *Chem. Mater.* **2004**, *16*, 1480–1484.
- (12) Kramer, S.; Fuierer, R. R.; Gorman, C. B. *Chem. Rev.* **2003**, *103*, 4367–4418.
- (13) Lee, K.-B.; Lim, J.-H.; Mirkin, C. A. *J. Am. Chem. Soc.* **2003**, *125*, 5588–5589.
- (14) Jung, H.; Kulkarni, R.; Collier, C. P. *J. Am. Chem. Soc.* **2003**, *125*, 12096–12097.
- (15) Barsotti, R. J., Jr.; O’Connell, M. S.; Stellacci, F. *Langmuir* **2004**, *20*, 4795–4798.

- (16) Mueller, W. T.; Klein, D. L.; Lee, T.; Clarke, J.; McEuen, P. L.; Schultz, P. G. *Science* **1995**, *268*, 272–273.
- (17) Blackledge, C.; Engbretson, D. A.; McDonald, J. D. *Langmuir* **2000**, *16*, 8317–8323.
- (18) Blasdel, L. K.; Banerjee, S.; Wong, S. S. *Langmuir* **2002**, *18*, 5055–5057.
- (19) Peter, M.; Li, X.; Huskens, J.; Reinhoudt, D. N. *J. Am. Chem. Soc.* **2004**, *126*, 11684–11690.
- (20) Suzuki, A. *J. Chem. Soc., Chem. Commun.* **2005**, 4759–4763.
- (21) Li, Y.; El-Sayed, M. A. *J. Phys. Chem. B* **2001**, *105*, 8938–8943.

Scheme 1. Schematic Representations of (Top) the Suzuki Reaction Initiated on the Aryl Bromide Monolayer by a PVP-Pd Nanoparticle-Coated AFM Probe, in a Methanolic Solution of 3-Aminophenylboronic Acid and Sodium Acetate, and (Bottom) a Probe-Mediated Aryl Styrene Heck Reaction



the synthesis of pharmaceuticals.²² The reagents are also typically air and water stable.²³

The Heck reaction, another of the many carbon–carbon coupling reactions catalyzed by palladium, involves the olefination of aryl halides in producing functionalized olefins and is a key reaction in the industrial-scale synthesis of natural products and pharmaceuticals.^{24,25} Historically, the palladium catalysts used are often phosphine or phosphane complexes. Although these stabilize the catalytically active Pd(0) formed in situ, these complexes typically have a low associated stability, and problems are accordingly encountered with the formation of catalytically inactive “palladium black”.²⁶ Recently, (stable) palladium nanoparticles have been shown to catalyze the Heck reaction.^{27–29} Polyvinyl-pyrrolidone-modified palladium (PVP-

Pd) nanoparticles have been shown to be stable in both air and water and to adhere robustly to silicon nitride surfaces.^{30,31}

We describe herein the application of suitably functionalized catalytically active AFM probes to the spatially localized induction of Heck and Suzuki aryl coupling reactions (Scheme 1). In many cases, measurable height changes induced by molecular coupling fall within the surface roughness of the reagent SAM, and the reaction is not characterizable by direct near-field topographical imaging. We have carried out exhaustive control reactions and characterized the surface by in-situ lateral force microscopy and functional-group-specific near-field topographic and far-field fluorescence imaging methods.

Results and Discussion

Monolayer Formation and Characterization. Surface-assembling terminal aryl halides (4-bromo/iodo-*N*-(3-(methylthio)propyl)benzamide) and a styrene (*N*-(3(methylthio)propyl)-4-vinylbenzamide) were synthesized as described (see Experimental Methods), assembled, and characterized by AFM, XPS, FTIR, and electrochemistry. XPS peaks due to N (1s), C

(22) Zenk, R.; Partzsch, S. *Chim. Oggi* **2003**, *21*, 70–73.

(23) Deng, Y.; Gong, L.; Mi, A.; Liu, H.; Jiang, Y. *Synthesis* **2003**, 337–339.

(24) Belatskaya, I. P.; Cheprakov, A. V. *Chem. Rev.* **2000**, *100*, 3009–3066.

(25) Danishevsky, S. J.; Masters, J. J.; Young, W. B.; Link, J. T.; Snyder, L. B.; Magee, T. V.; Jung, D. K.; Bornmann, R. C. A. I. W. G. *J. Am. Chem. Soc.* **1996**, *118*, 2843–2859.

(26) Amatore, C.; Jutand, A. *Acc. Chem. Res.* **2000**, *33*, 314–321.

(27) Reetz, M. T.; Breinbauer, R.; Wanninger, K. *Tetrahedron Lett.* **1996**, *37*, 4499–4502.

(28) Gniewek, A.; Trzeciak, A. M.; Ziolkowski, J. J.; Kepinski, L.; Wrzyszczyk, J.; Tylus, W. *J. Catal.* **2005**, *229*, 332–343.

(29) Bhattacharya, S.; Srivastava, A.; Sengupta, S. *Tetrahedron Lett.* **2005**, *46*, 3557–3560.

(30) Boonekamp, E. P.; Kelly, J. J.; Fokkink, L. G. J. *Langmuir* **1994**, *10*, 4089–4094.

(31) Boonekamp, E. P.; Kelly, J. J.; Fokkink, L. G. J.; Vandenhout, D. W. E. *J. Electrochem. Soc.* **1995**, *142*, 519–524.

(1s), and Br (3d) were observed at the same binding energies as equivalent peaks in the raw material. Specific data points for the aryl halide SAMs were as follows: Br (3d_{5/2}, 3d_{3/2}) 70.8, 71.6 eV; S (2p_{3/2}, 2p_{1/2}) 163.3, 162.2 eV; C (1s) 285.0 eV; C (1s, amide) 287.8 eV; N (1s) 399.7 eV. In both the monolayer and the raw material samples, there is a carbon 1s peak at ~288 eV, attributed to the amide carbon. The bromine doublet in the spectrum of the monolayer is weak as expected from its population on the surface. The position of the sulfur 2p doublet had shifted to lower energy by ~1.3 eV as compared to the unbound sulfur of the raw material. Although the mode of dialkylsulfide surface assembly remains unclear, this shift is both indicative of the presence of a thiolate species (with associated C–S bond cleavage) and consistent with the mechanical stability of these SAMs (see below). The *N*-(3-(methylthio)propyl)-4-benzamide styrene SAM XPS peaks were observed as S (2p_{3/2}, 2p_{1/2}) 163.0, 161.8 eV; C (1s) 285.0 eV; C (1s, amide) 288.0 eV; N (1s) 399.9 eV.

The amide A and B resonances (N–H stretch and associated Fermi resonance) in the solid state were absent from grazing FTIR spectra of the monolayer, consistent with the N–H bonds being parallel to the surface and intermolecularly hydrogen-bonded.^{32–34} In the monolayer sample, amide III appears at 1265 cm⁻¹, in accordance with literature values.^{32,34} Amide II appears in the same region as the water bend and is, therefore, obscured. In polarization modulated spectra, it was resolved at 1543 cm⁻¹.^{35,36} Amide I is not seen, even when a moving average is placed through the data. The presence and absence of these two peaks is also indicative of hydrogen bonding, with the NH and CO bonds parallel to the surface, and a trans arrangement of the amide bond.³⁷ Additional resonances due to the methylene, C–C, and para-substituted benzene rings were also resolved as expected.³⁴ Molecular coverages were determined, by stripping voltammetry, to be (2.0–3.0) × 10¹⁴ and (2.0–2.5) × 10¹⁴ molecules cm⁻² for the aryl halide and styrene adlayers, respectively.

Mechanical Nanolithography and Nanografting. To ascertain both likely limits of lateral resolution and the limits of vertical force that could be nondestructively imparted to the reagent SAM, force tolerances were obtained by lithographic scanning under MilliQ water (18.2 MΩ). This was performed at a high scan rate (between 40 and 60 Hz) over an area of 400 nm and at force that was increased stepwise until successful mechanical lithography was achieved. The dialkylsulfide adlayers exhibited the same mechanical stability as analogous alkanethiol SAMs; they were stable up to 70 ± 5 nN of applied force, beyond which the adsorbate is removed and the resulting hole depth measured at low (noncompressional force) to be that associated with an all-trans molecular configuration and a tilt angle of 25–30°.

Nanografting experiments were carried out to verify the feasibility of tagging and locating introduced highly localized functional groups. Optimal tip velocities were found to be in

the region of 1 μm/s, a magnitude that translates into a tip–molecule contact time of some 5.6 ms being required to achieve substitution, derived using a Hertz model.³⁸ The grafting of lipoic or mercaptohexadecanoic acid into alkylthiol monolayers could be followed by subsequent tagging with an acid reactive fluorophore, Alexafluor 488 hydrazide (see Supporting Information).

AFM-Driven Reactions. It was envisaged that the GPa pressure developed beneath an AFM probe would facilitate efficient Suzuki coupling at room temperature. With palladium film-coated probes, however, no evidence for reaction was observed. This can be ascribed either to the wearing away of the metal layer upon scanning, or the comparatively lower number of catalytic sites offered to the halogenated surface.³⁹ Although the activity of catalytic nanoparticles can be a sensitive function of size, shape, and surface modification,⁴⁰ it is generally found to be high, an observation broadly assigned to their high surface area:volume ratio.^{27,39,41–44} Colloidal particle-mediated Heck coupling has, for example, been observed to be more facile than the initial “industry standard” of palladium on activated carbon.⁴² Both Suzuki and Heck couplings have also been extensively catalyzed through the use of phosphine-ligated palladium complexes.^{45,46} We have found no precedent for the successful use of evaporated (“planar”) metallic in these reactions. (Although there are many examples of ligandless palladium catalysts in these reactions, these are immobilized on high surface area supports such as activated carbon.^{47,48}) PVP-Pd nanoparticles are known to adhere to silicon nitride and to catalyze Suzuki reactions in aqueous solution.^{49–51} There is also some precedent for their application to Heck catalysis.^{27,28} They were prepared from poly(vinylpyrrolidone) (PVP) with a molecular weight of 40 000, imaged by AFM, and their activity assessed in fluid-phase Suzuki and Heck coupling reactions, using reagents subsequently employed in the probe-driven reaction.

Surface-confined Suzuki reactions were initiated by scanning a SAM of 4-bromo/iodo-*N*-(3-(methylthio)propyl)benzamide with a PVP-Pd nanoparticle-functionalized AFM probe at a force of 15–25 nN and a speed of 1 μm/s in a methanolic solution of sodium acetate and 3-aminophenylboronic acid. For the Heck reaction, a SAM of *N*-(3-(methylthio)propyl)-4-vinylbenzamide was scanned with an equivalent probe at a force of 25–40 nN at a speed of 2 μm/s in a DMF solution of sodium hydrogen carbonate and 4-iodobenzoic acid. This process catalyzes the

- (32) Yu, H.-Z.; Ye, S.; Zhang, H.-L.; Uosaki, K.; Liu, Z.-F. *Langmuir* **2000**, *16*, 6948–6954.
 (33) Clegg, R. S.; Hutchison, J. E. *Langmuir* **1996**, *12*, 5239–5243.
 (34) Lenk, T. J.; Hallmark, V. M.; Hoffmann, C. L.; Rabolt, J. F.; Castner, D. G.; Erdelen, C.; Ringsdorf, H. *Langmuir* **1994**, *10*, 4610–4617.
 (35) Zamylny, V.; Zawisza, I.; Lipkowski, J. *Langmuir* **2003**, *19*, 132–145.
 (36) Barner, B. J.; Green, M. J.; SBez, E. I.; Corn, R. M. *Anal. Chem.* **2001**, *63*, 55–60.
 (37) Tam-Chang, S.-W.; Biebuyck, H. A.; Whitesides, G. M.; Jeon, N.; Nuzzo, R. G. *Langmuir* **1995**, *11*, 4371–4382.

- (38) Schwarz, U. D. *J. Colloid Interface Sci.* **2003**, *261*, 99–106.
 (39) Narayanan, R.; El-Sayed, M. A. *J. Am. Chem. Soc.* **2003**, *125*, 8340–8347.
 (40) Bonnemann, H.; Braun, G. A. *Angew. Chem., Int. Ed. Engl.* **1996**, *35*, 1992–1995.
 (41) Beller, M.; Fischer, H.; Kuhlein, K.; Reisinger, C. P.; Herrmann, W. A. *J. Organomet. Chem.* **1996**, *520*, 257–259.
 (42) Dhas, N. A.; Gedanken, A. *J. Mater. Chem.* **1998**, *8*, 445–450.
 (43) Yeung, L. K.; Crooks, R. M. *Nano Lett.* **2001**, *1*, 14–17.
 (44) Bradley, J. S. In *Clusters and Colloids*; Schmid, G., Ed.; VCH: Weinheim, 1994; Chapter 6.
 (45) Meijere, A. d.; Meyer, F. E. *Angew. Chem., Int. Ed. Engl.* **1995**, *33*, 2379–2411.
 (46) Cabri, W.; Candiani, I. *Acc. Chem. Res.* **1995**, *28*, 2–7.
 (47) Mukhopadhyay, S.; Rothenberg, G.; Joshi, A.; Baidossi, M.; Sasson, Y. *Adv. Synth. Catal.* **2002**, *344*, 348–354.
 (48) Prekl, S. S.; Kleist, W.; Khler, K. *Tetrahedron* **2005**, *61*, 9855–9859.
 (49) Van der Putten, A. M. T.; De Bakker, J. W. G.; Fokkink, L. G. J. *J. Electrochem. Soc.* **1992**, *139*, 3475–3480.
 (50) Li, Y.; Hong, X. M.; Collard, D. M.; El-Sayed, M. A. *Org. Lett.* **2000**, *2*, 2385–2388.
 (51) Narayanan, R.; El-Sayed, M. A. *J. Phys. Chem. B* **2004**, *108*, 8572–8580.

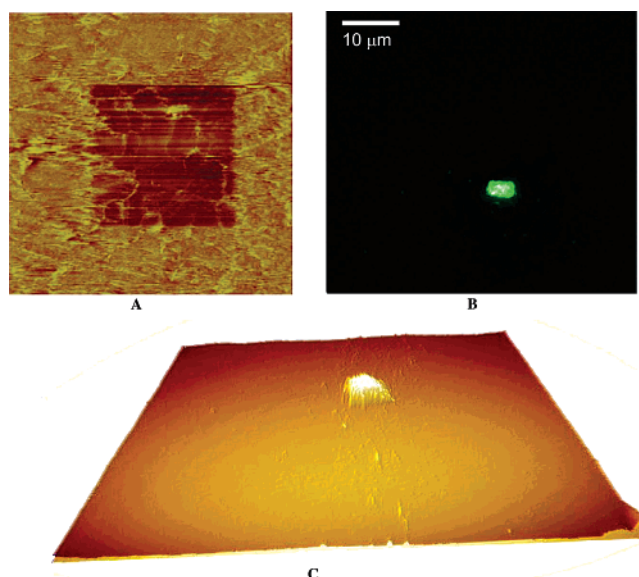


Figure 1. (A) A subtracted friction image of a localized ($3 \mu\text{m}$ square) Suzuki coupling between an aryl bromide reagent SAM and 3-aminophenylboronic acid. The change from a higher to a lower contrast may be a consequence of the catalytic probe having a higher free energy interaction with the unreacted aryl bromide-terminating component of the SAM (which will be attempting to oxidatively add). The (geometric) change in height during the reaction is expected to be $3.0\text{--}3.5 \text{ \AA}$,⁶⁰ which is less than that reliably detectable by a finite radius AFM probe, taking into account the limitations of tip convolution and the thermal noise at room temperature. As expected, then, no change is seen in the topographic image. (B) Epifluorescence image (488 nm excitation) of a $4.5 \times 2.25 \mu\text{m}$ patch of Suzuki-generated amine-terminated SAM. The chemical specificity of the dye tag facilitates a low background emission. (C) A fluid phase $30 \mu\text{m}$ topographic AFM image showing a central $5 \times 5 \mu\text{m}$ SAM patch tagged with 100 nm aldehyde-functionalized nanospheres.

coupling of the aryl bromide/iodide to the terminal styrene moiety of the SAM.

After the monolayer was scanned with the catalytic probe, forces were minimized. The scan rate was then increased to approximately $5\text{--}10 \mu\text{m s}^{-1}$, and the scan size increased. It is possible, in this way, to characterize (by chemical force imaging; see below) the generated pattern in situ without initiating further reaction.

Free energies at atomically flat interfaces are controlled by the chemical functional groups at the surface of the substrate. This gives rise to frictional force-mediated lateral tip deflections during scanning according to

$$f = \alpha F_N + f_0$$

where f is frictional force, α and f_0 are constants related to the chemical composition of the end-groups at the surface, and F_N is the total normal force, that is, the sum of capillary forces, molecular interactions, and applied lever load. With the feedback loop keeping the normal force constant during scanning, the variant frictional force maps the SAM surface free energy.⁵² If the trace and retrace friction images are subtracted, an image representing the surface free energy, with no contribution from inhomogeneities in the surface topography, is produced (Figure 1A).

Aryl couplings could be initiated, at a success rate of $\sim 80\%$ (based on a statistical analysis of attempted reactions and those deemed, by subsequent imaging analyses, to be successful) and

in a single sweep of the surface, at probe scan rates of between 0.04 and $4.5 \mu\text{m s}^{-1}$. Reaction could, additionally, be induced at scan rates of up to $9 \mu\text{m s}^{-1}$ but at decreasing yield and only on repeated passes of the catalytic tip over the reagent adlayer. Coupling reactions could be similarly induced using 3-aminophenylboronic acid at line widths down to $10\text{--}15 \text{ nm}$. Although the topographic and frictional contrast characteristics induced in the reagent adlayer are consistent with those expected on successful aryl coupling, these localized changes can be additionally confirmed by chemically specific labeling (Figure 1B,C). Subsequent topographic or emission mapping confirms the localization of these amine-specific labels only in surface areas initially defined by the scan parameters used during reaction induction. Carboxylate moieties introduced by catalytically scanning the aryl styrene SAM were tagged with Alexa Fluor 488 hydrazide.

Rigorous control experiments were carried out to verify that the surface optical, topographic, and frictional changes outlined were the direct result of AFM probe-immobilized palladium nanoparticle aryl–aryl coupling and not associated with, for example, disruption of the reagent SAM.¹⁹ A 30-fold repeat of the outlined Suzuki procedure in the absence of the solution-phase boronic acid reagent led to no observations of topographic, frictional, or optical change. A 30-fold repeat with a non-nanoparticle-coated AFM probe in the presence of all reagents similarly leads to no detectable surface chemical changes. In both cases, surface patterning only occurs with nanoparticle-modified probes (not evaporated film) and only within a specified rate and force window.

In a similar manner, it is possible to induce and control Heck coupling between a surface-confined aryl styrene and a solution-phase aryl halide with equivalently prepared catalytic palladium AFM probes (Figures 2 and 3). By appropriate fine control of the probe path, molecular coupling could be directed in any prescribed pattern with line widths down to (a probe radius limited) ~ 20 molecules (Figure 4). [Reactions could be driven using probes prepared and stored under ambient conditions for up to 3 days. XPS analyses of the particles indicated a good stability to oxidation within this time frame (see Supporting Information).]

In making the simplifying assumption that the catalytic probe has the same radius of curvature as the unmodified silicon nitride tip (35 nm radius), the Hertz model can be used to estimate the contact area between it and the underlying planar substrate.³⁸ [This model, originating from the work of Hertz⁵³ to explain the (elastic) deformation of contacting bodies, has been successfully applied in original and modified forms to a consideration of the mechanics within AFM junctions.^{54,55}] The presence of the monolayer, modification of tips, and interfacial energies acting at the surface are not taken into account. Using this model, for an applied force of 20 nN , values of 2 and 13 nm^2 are obtained for the contact radius and area, respectively.³⁸ These values, in conjunction with an electrochemically derived surface coverage and the typical reaction-initiating scan speed, lead to a turnover number (TON) per probe of 0.7×10^4 molecules s^{-1} (0.1 zeptomoles s^{-1}) (assuming 100% reagent conversion). This may be compared to previously determined

(53) Hertz, H. J. *Reine Angew. Math.* **1882**, *92*, 156–171.

(54) Domke, J.; Radmacher, M. *Langmuir* **1998**, *14*, 3320–3325.

(55) Rotsch, C.; Jacobson, K.; Radmacher, M. *Proc. Natl. Acad. Sci. U.S.A.* **1999**, *96*, 921–926.

(52) Leggett, G. J. *Anal. Chim. Acta* **2003**, *479*, 17–38.

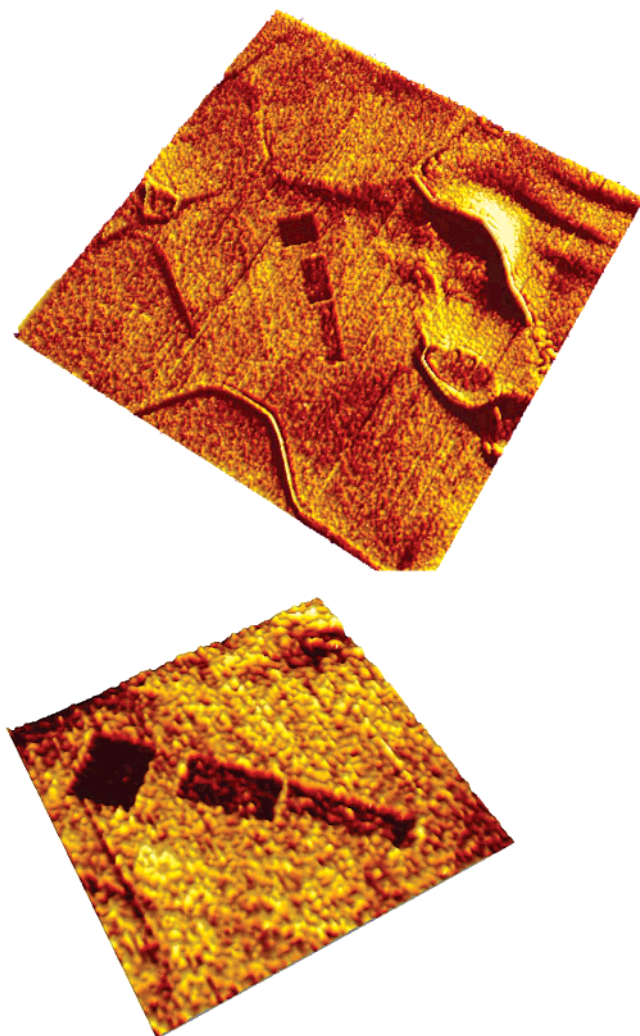


Figure 2. Surface friction maps of a Heck patterned adlayer on an evaporated gold film/reagent SAM surface. The coupling reaction was carried out at 22 °C, at 30 nN of force, and probe sweep rates of 3–4 $\mu\text{m s}^{-1}$. The three product patches are (left to right) 200 \times 200 nm (8×10^4 molecules driven at 3.0 $\mu\text{m s}^{-1}$), 300 \times 150 nm (9×10^4 molecules driven at 3.5 $\mu\text{m s}^{-1}$), and 400 \times 100 nm (8×10^4 molecules driven at 4.0 $\mu\text{m s}^{-1}$). The decreasing contrast with increasing probe scan rate is evident in the lower figure and reflects rate capping as probe speeds reach 4.0 $\mu\text{m s}^{-1}$.

TONs associated with the use of solution-phase, ligand-stabilized, palladium catalysts.⁵⁶ The equivalent calculation for the surface-driven Heck reactions gives a TON of (4–4.7) $\times 10^4$ molecules s^{-1} . Although these values lie toward the low end of those achieved in solution, one may consider them to be high bearing in mind the diffusion restrictions inherent in not only confining one of the reagents to a surface but also demanding that the other access the confined tip–substrate volume. In the case of the Suzuki reaction, it is instructive to compare the observed reaction rate limitations associated with both the iodide and the bromide functionalities. With the bromide termination, the reaction appears to be effective at probe scan rates up to 8 $\mu\text{m s}^{-1}$. With the iodide-terminated reagent, however, reaction efficiency (assessed by decreasing chemical force contrast) drops off rapidly at sweep rates exceeding 3 $\mu\text{m s}^{-1}$ (see Supporting Information). These observations are “reversible” in the sense that a decrease in rate restores the

(56) Bellina, F.; Carpita, A.; Rossi, R. *Synthesis* **2004**, 15, 2419–2440.



Figure 3. Heck-mediated aryl couplings patterned in the form of a Japanese emoticon. All dimensions are in nanometers.

effectiveness of turnover. Although the mechanistic details of the Suzuki reaction are unclear, it is believed that the rate-determining steps are reductive elimination and oxidative addition in the case of the aryl iodide and bromide, respectively.⁵⁷ One may hypothesize that, within the GPa confined space associated with the probe-catalyzed reaction, the rate at which the active metal surface is replenished by reductive elimination (of both the coupled product and the boron halide) will be limiting in both cases. The faster rate of reaction observed here with the bromide may then reflect its more enthalpically favorable bonding to the boron.

Conclusions

The site-specific Suzuki and Heck coupling of solution-phase and surface-assembled reagents by a scanning catalytic probe has been demonstrated. The spatially localized introduction of terminal amine, phenyl, or carboxylate moieties can be verified by fluorescent tagging, frictional imaging, and labeling with suitably functionalized nanoparticles where appropriate. “Reaction-writing” line widths down to 12–15 nm are possible and can be confined to turn over subzeptomolar levels of substrate. Through appropriate control of the scanning catalyst, it is possible to “write” coupling reactions in an essentially unlimited way and with line widths of only 20 or so molecules (limited by probe and catalyst finite size). In calibrating probe–reagent interaction time, surface-confined turnover numbers can be determined. In modulating interaction times, the rates of reaction

(57) Lioubashevski, O.; Chegel, V. I.; Patolsky, F.; Katz, E.; Willner, I. *J. Am. Chem. Soc.* **2004**, 126, 7133–7143.

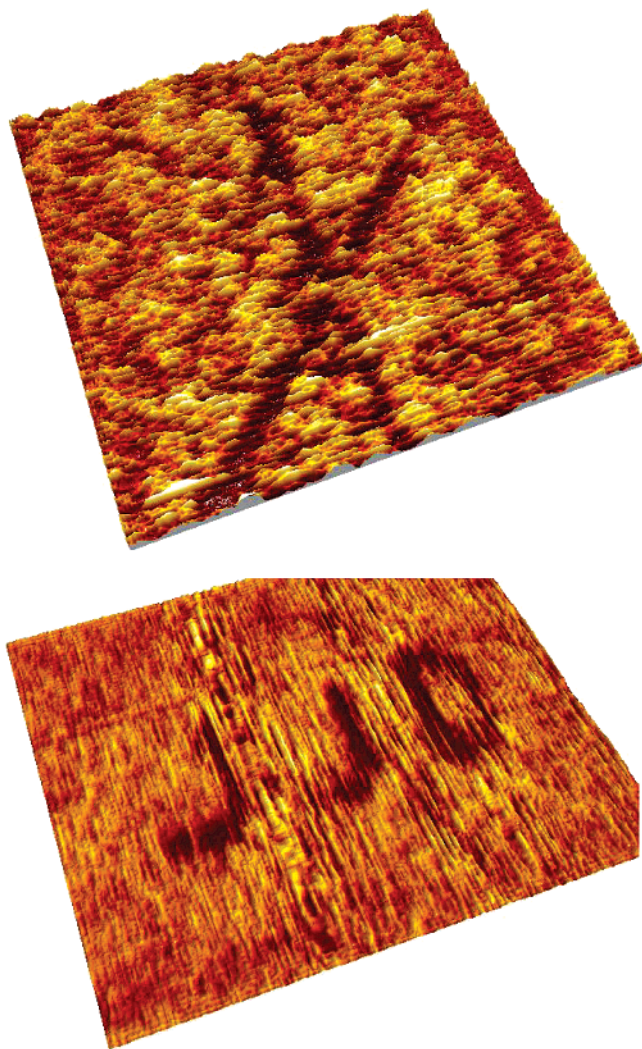


Figure 4. Friction image of a Heck patterned surface cross (top). Each line (scribed at an angle of 45° to each other) is 500 nm long and has a probe-limited width of 13 ± 3 nm or some 20 molecules. This reaction was carried out in dry DMF, 22°C , and at probe force and sweep rates of 40 nN and $1 \mu\text{m s}^{-1}$, respectively. Friction map of a Heck reaction in which aryl coupling has been patterned into the letters “JJD” (line widths ~ 25 nm).

are controllable but ultimately limited by diffusion of the second reagent from solution. In both coupling reactions, TONs of 10^4 molecules s^{-1} are possible. This work further highlights the prospects of using proximal probes to localize and control specific chemical reactions and, in so doing, direct molecular assembly.

Experimental Methods

NMR spectra were run on a 300 MHz Varian spectrometer. Mass spectrometry samples were run on a Micromass GCT mass spectrometer using a temperature-programmed solids probe inlet. Elemental analysis was carried out by the analytical services department at the University of Oxford, Inorganic Chemistry Laboratory. XPS experiments were carried out at The CCLRC Daresbury Laboratory, Cheshire, UK, using an ESCA300 spectrometer. It comprised a rotating anode X-ray source (titanium alloy disk operating at 4000 or 10 000 rpm), Al $K\alpha$ X-rays used in transmission mode, a quartz crystal monochromator, a high transmission/imaging lens, a hemispherical analyzer, and a multichannel detector. The vacuum in the analysis chamber was approximately 1×10^{-10} mbar. The slit width was 0.8 mm, and the takeoff angle was 90° . Analyses were performed on both monolayer samples and on powdered

samples of the raw materials. Peak positions of SAM and solid samples were compared by compensating for the effects of the flood gun operation by referencing all peaks to the C (1s) at 285.0 eV. AFM was performed using Nanoscope IIIa or Nanoscope IV Multimode atomic force microscopes, or a JPK Nanowizard atomic force microscope. The former were used in conjunction with either an E or J scanner, and a Digital Instruments glass fluid cell. Silicon nitride contact tips from Veeco were used in all experiments, with spring constants of 0.06 or 0.12 N/m. Palladium tips were fabricated by coating these probes with a 5 nm layer chromium adhesion layer and 22 or 45 nm of palladium. Fluorescence imaging was carried out with a Nikon Eclipse TE2000-U inverted optical and epi-fluorescence microscope used in conjunction with an Ixon Andor ICCD back illuminated, air cooled camera, with appropriate excitation and emission filters.

All reagents were used as received: methanol (HPLC grade, Rathburn), 4-bromobenzoic acid (98%, Aldrich), 4-iodobenzoic acid (Aldrich, 98%), 3-(methylthio)propylamine (97%, Acros), PS-carbodiimide (Argonaut Technologies), anhydrous sodium acetate (99.0%, BDH), 3-aminophenylboronic acid (98%, Aldrich), 4-vinylbenzoic acid (Aldrich, 97%), NHS-fluorescein (Pierce), Alexa Fluor 488 Hydrazide (Molecular Probes), gold on glass (11 mm \times 11 mm, Arrandee), and aldehyde-functionalized nanospheres (100 nm diameter, Brookhaven Ltd.).

Synthesis of (4-Bromo-*N*-(3-(methylthio)propyl)benzamide. Two equivalents of PS-carbodiimide (*N*-cyclohexylcarbodiimide-*N*-propyloxymethyl polystyrene) and 1.5 equiv of 4-bromobenzoic acid were stirred in dry dichloromethane for 5 min. Next, 1 equiv of 3-(methylthio)propylamine was added and stirred at room temperature under nitrogen for 18 h. After the mixture was filtered and washed with dry dichloromethane, the solvent was removed under vacuum to afford the coupled product. $^1\text{H NMR}$ (CDCl_3): δ 7.52 (q, 4H), δ 6.71 (s, 1H), δ 3.47 (q, 2H), δ 2.52 (t, 2H), δ 2.04 (s, 3H), δ 1.85 (m, 2H). $^{13}\text{C NMR}$ (CDCl_3): δ 166.83, δ 133.56, δ 131.96, δ 128.76, δ 126.29, δ 39.69, δ 32.20, δ 28.49, δ 15.73. Anal. Calcd: C, 45.84; H, 4.89; N, 4.86. Found: C, 45.88; H, 4.90; N, 4.91. MS solid probe EI, 286.9974; found, 286.9979. XPS peaks for the raw material, referenced to the carbon 1s peak at 285.0 eV; C (1s) 285.0 and 288.0 eV (amide), N (1s) 399.9 eV, S ($2p_{3/2}$, $2p_{1/2}$) 163.5 and 164.8 eV, Br ($3d_{3/2}$, $3d_{1/2}$) 71.0 and 71.1 eV.

Synthesis of *N*-(3-(Methylthio)propyl)-4-vinylbenzamide. Two equivalents of PS-carbodiimide (*N*-cyclohexylcarbodiimide-*N*-propyloxymethyl polystyrene) and 1.5 equiv of 4-vinylbenzoic acid were stirred in dry dichloromethane for 5 min. Next, 1 equiv of 3-(methylthio)propylamine was added and stirred at room temperature under nitrogen for 18 h. After the mixture was filtered and washed with dry dichloromethane, the solvent was removed under vacuum to afford the coupled product. $^1\text{H NMR}$ (CDCl_3): δ 7.67 and 7.40 (AA'BB', Ph, 4H), δ 6.7 (m, 1H), δ 6.40 (s, 1H), δ 5.78 (d, 1H), δ 5.29 (d, 1H), δ 3.52 (q, 2H), δ 2.55 (t, 2H), δ 2.06 (s, 3H), δ 1.88 (m, 2H). $^{13}\text{C NMR}$ (CDCl_3): δ 167.4, δ 140.7, δ 136.2, δ 133.8, δ 127.6, δ 126.6, δ 116.1, δ 39.5, δ 32.2, δ 28.7, δ 15.7. Anal. Calcd: C, 66.38; H, 7.23; N, 6.00. Found: C, 64.4; H, 7.57; N, 6.00. MS solid probe EI, 235.1031; found, 235.1029. XPS peaks for the raw material, referenced to the carbon 1s peak at 285.0 eV; C (1s) 285.0 and 288.0 eV, N (1s) 399.9 eV, S ($2p_{3/2}$, $2p_{1/2}$) 163.5 and 164.6 eV. To form SAMs of the aryl bromide or styrene, a 1 mM methanolic solution of the compound was prepared. Subsequently annealed gold on glass was immersed in the solution overnight. The sample was then rinsed with methanol, blown dry with nitrogen, and used immediately.

Synthesis of Polyvinyl Pyrrolidone-Stabilized Palladium Nanoparticles. The PVP-Pd nanoparticles were synthesized using a previously described procedure.^{58,59} 177.4 mg (1.0 mmol) of $[\text{PdCl}_4]^{2-}$ (Aldrich 99%) was dissolved in 10 mL of 0.2 M hydrochloric acid

(58) Teranishi, T.; Miyake, M. *Chem. Mater.* **1998**, *10*, 594–600.

(59) Choo, H. P.; Liew, K. Y.; Liu, H. *J. Mater. Chem.* **2002**, *12*, 934–937.

(60) Han, T.; Beebe, T. P. *Langmuir* **1994**, *10*, 2705–2709.

(BDH, analar) and made up to 500 mL with water, making a 2 mM solution. The mixture was sonicated until all of the solid had dissolved. 15 mL of the 2 mM solution was added to a 40% ethanol/water mixture in a round-bottomed flask. 38.5 mg (1 μ mol) of poly(vinylpyrrolidone) (Sigma, molecular weight: 40 000) was added to the flask and heated to reflux for 3 h. The spectral changes accompanying reduction of $[\text{PdCl}_4]^{2-}$ to Pd(0) were monitored using UV–visible spectroscopy (see Supporting Information).⁵⁰ The resulting PVP-Pd nanoparticle solution was stored under nitrogen until use.

AFM-Driven Suzuki Coupling. Silicon nitride contact AFM probes were modified by first treating them for 30 min in a Bioforce UV-tip cleaner, and then incubating them in an aqueous solution of the PVP-Pd nanoparticles for 5 min,⁵⁸ then 1 min, then 30 s, drying with nitrogen between each coating step. In later work, a more robust modification could be achieved by incubating clean AFM probes in the refluxing PVP-Pd solution during nanoparticle preparation. Probes were removed, dried under nitrogen, and stored in air for up to 1 week prior to use.

The aryl bromide dialkyl sulfide-modified gold surface was mounted onto an AFM sample plate and a defined area scanned once using the catalytic tip at speeds between 0.04 and 4.5 $\mu\text{m/s}$, with a force of 15–25 nN. During scanning, the probe and substrate were incubated in a millimolar methanolic (or 4:1 v/v methanol/water) solution of 3-aminophenylboronic acid (or 4-carboxyphenylboronic acid) and sodium acetate. After reaction, the scan size was increased, the force minimized, and the scan rate increased to image the area with the same probe without inducing further reaction.

AFM-Driven Heck Coupling. A silicon nitride 0.12 N/m AFM probe, previously incubated in a solution of PVP-Pd nanoparticles (~ 1.4 M in Pd), was used to scan the styrene SAM in a DMF solution of 2 mM 4-iodo/bromo-benzoic acid and 8 mM sodium hydrogen carbonate. Scan rates of 2 $\mu\text{m/s}$ and forces of greater than 25 nN were used to induce the reaction. To obtain friction images that result only from lateral deflections of the tip and not topographic contributions, the forward and reverse scans were saved separately and subtracted from one another.⁵²

Optical and Topographic Amine Tagging. The monolayer sample was sonicated and rinsed in methanol, then incubated in pH 7.0, 20 mM phosphate buffer solution prior to the addition of 1 mg of 5-(6-carboxyfluorescein succinimidyl ester (“NHS-fluorescein”) in 10 μL of DMF for 2 h in the dark. The surface was rinsed copiously prior to optical imaging. Topographic tagging was achieved through a 2 h surface incubation with a sonicated 0.1% aqueous aldehyde nanosphere suspension followed by copious rinsing and fluid phase contact AFM imaging.

Optical Tagging of Heck-Introduced Carboxylate Functionalities.

After AFM scanning as described, and copious surface rinsing/sonication in methanol, carboxylate tagging was carried out using a solution comprising EDC (9.4 mM) in water, to which 10 μL of a 10 mM stock solution of Alexa Fluor 488 hydrazide was added.

Suzuki Reaction in Solution. 4-Bromobenzoic acid (40 mg, 0.2 mmol), 3-aminophenylboronic acid (47 mg, 0.3 mmol), and sodium acetate (49 mg, 0.6 mmol) were dissolved in 20 mL of 40% ethanol. Once boiling, 2 μL of PVP-Pd colloid solution was added, and the mixture was refluxed for 18 h. The solvent was then removed, and the resultant off-white powder was analyzed by mass spectrometry.

Heck Reaction in Solution. 74 mg (0.5 mmol) of 4-vinylbenzoic acid, 121 mg (0.6 mmol) of 4-bromobenzoic acid, and 210 mg (2.5 mmol) of sodium hydrogen carbonate were dissolved in 10 mL of DMF. 1 μL of a solution of PVP-stabilized palladium nanoparticles was added,⁵⁸ and the mixture was refluxed at 100 $^\circ\text{C}$ for 7 h. After reaction, the solvent was removed and the product was analyzed by mass spectrometry.

Nanografting experiments were carried out to test the reliability of tagging localized introduced specific chemical functionalities. Nanografting was performed using the AFM apparatus setup for contact imaging in fluid. Initial low (< 1 nN) force imaging of alkythiol SAMs was followed by localized scanning at higher force (~ 60 nN; $0.5 \mu\text{m s}^{-1}$), in a 1 mM solution of lipoic acid, octadecanethiol, or mercapto-hexadecanoic acid, and subsequent re-imaging of the region at low force.

Acknowledgment. We acknowledge financial support from the Engineering and Physical Sciences Research Council (EPSRC), Dr. G. Beamson of the Surface and Nuclear Division, Daresbury Laboratory, UK, for help with XPS, and Mrs. H. Burgess for assistance with the fluorescence imaging.

Supporting Information Available: SAM force tolerance data, nanografting, Suzuki coupling, scan rate dependence data, friction imaging cross-section analysis, preparation and characterization of poly(vinylpyrrolidone) palladium nanoparticles, and derivation of tip–molecule contact area. This material is available free of charge via the Internet at <http://pubs.acs.org>.

JA064840A